Hydrogen Bonding in Phenol, Water, and Phenol−Water Clusters

R. Parthasarathi,[†] V. Subramanian,*[,†] and N. Sathyamurthy*[,‡]

Chemical Laboratory, Central Leather Research Institute, Adyar, Chennai, India 600 020 and Department of Chemistry, Indian Institute of Technology, Kanpur, India 208 016

Received: August 4, 2004; In Final Form: October 29, 2004

Structure, stability, and hydrogen-bonding interaction in phenol, water, and phenol−water clusters have been investigated using ab initio and density functional theoretical (DFT) methods and using various topological features of electron density. Calculated interaction energies at MP2/6-31G* level for clusters with similar hydrogen-bonding pattern reveal that intermolecular interaction in phenol clusters is slightly stronger than in water clusters. However, fusion of phenol and water clusters leads to stability that is akin to that of H_2O clusters. The presence of hydrogen bond critical points (HBCP) and the values of $\rho(r_c)$ and $\nabla^2\rho(r_c)$ at the HBCPs provide an insight into the nature of closed shell interaction in hydrogen-bonded clusters. It is shown that the calculated values of total $\rho(r_c)$ and $\nabla^2\rho(r_c)$ of all the clusters vary linearly with the interaction energy.

Introduction

Studies on hydrogen bonding in several model systems have been carried out over the years, with a view to understand various chemical and biochemical processes in real life systems.[1,2] Numerous experimental and theoretical studies have been undertaken on a variety of small molecular clusters to probe solvation phenomena, as solvation effects play an important role in defining structural and functional aspects of biological macromolecules.[1−9] Substantial advances in molecular modeling and experimental techniques in recent years have made it possible to obtain a finer level of understanding of the hydrogen-bonding interaction in a variety of molecular clusters.[3] Supersonic molecular beam techniques have enabled the study of size-selected gas-phase molecular clusters and have provided molecular level insight into the bulk properties.[3−19] The double-resonance laser spectroscopic techniques have provided structural information on various molecular clusters.[13] Ab initio calculations at different levels of theoretical rigor have been carried out to explore the structure, stability, and strength of hydrogen bonding in these clusters. Three thematic issues of one review journal have been devoted to the properties of van der Waals (vdW) clusters.[3−8] In an earlier paper, we have reported on the structure and stability of water clusters (W_n) of size up to $n = 20$.[20] Very recently, alternative models for the dynamics of low-energy states of water trimer have been addressed using a simple perturbation treatment, which reproduces the experimental results.[21] The hydration patterns for aldehydes and amides have been explored with the help of ab initio calculations by examining the electrostatic topographical features.[22] Jordan and collaborators have made seminal contributions in understanding the structure of water clusters in organic hosts, various structural motifs in water cluster interactions with small molecules, and also on graphite surfaces, using both theoretical and experimental methods.[23]

Similar to water molecules, phenol (P) molecules can interact with each other and also with water molecules to form hydrogen-bonded clusters. Since phenol is the simplest aromatic alcohol and has the chromophore of an aromatic amino acid, hydration of phenol molecules has been studied as a natural first step to understand hydrogen bonding that represents solute−solvent interaction in biological systems. Studies on phenol−water (PW) clusters have shed much light on the geometries of the clusters and the nature of hydrogen bonding therein.[10,24−39] Various theoretical and experimental studies have revealed that the hydrogen bonding in PW clusters is similar to that of W_n.[10,24−39] Structure and stability of the hydrogen-bonded complexes of one phenol molecule with one to four water molecules have been investigated at various levels of ab initio theory by Dimitrova.[35] His studies revealed that for complexes with two, three, and four water molecules, the most stable structure was a planar ring. A second-order Møller−Plesset (MP2) perturbation theoretic study using interaction-optimized double-ζ plus polarization basis set has revealed the existence of three different minima in the phenol−water complex.[36] Benoit and Clary have studied phenol−water clusters using rigid-body diffusion quantum Monte Carlo method.[37,38] Earlier studies suggested that the interaction involved in PW clusters is similar in strength to the π-hydrogen bond.[36] Ab initio calculations have also been carried out for the electronic ground state and the lowest excited state of phenol and complexes of phenol with water and ammonia and the corresponding cations.[39]

Vibrational spectroscopy of phenol and phenol−water mixed clusters have suggested possible geometries for P_2 and P_3 and PW_n, where $n = 1-5$.[10] However, there is not much information available on the mixed clusters of the P_mW_n ($m > 1$) type. Since the participation of phenolic −OH group in hydrogen bonding is similar to that in water clusters, it is natural to expect the hydrogen-bonding pattern of phenol−water mixed clusters to be similar to that in water clusters. Hence, a systematic study has been undertaken to predict the geometries of P_mW_n ($m = 1-3$, $n = 1-3$, $m + n \leq 4$) clusters and to compare them with the corresponding geometries for W_2, W_3, W_4, P_2, P_3, and P_4.

The theory of atoms-in-molecules (AIM) allows one to understand the concept of a chemical bond and its strength in terms of electron density distribution.[40,41] The AIM theory utilizes the topological features of electron density (ρ) and

* Address correspondence to these authors. Tel: +91 44 24411630; fax: +91 44 24911589; e-mail: subuchem@hotmail.com, nsath@iitk.ac.in.
† Central Leather Research Institute.
‡ Indian Institute of Technology.

10.1021/jp046499r CCC: $30.25
Published on Web 01/15/2005

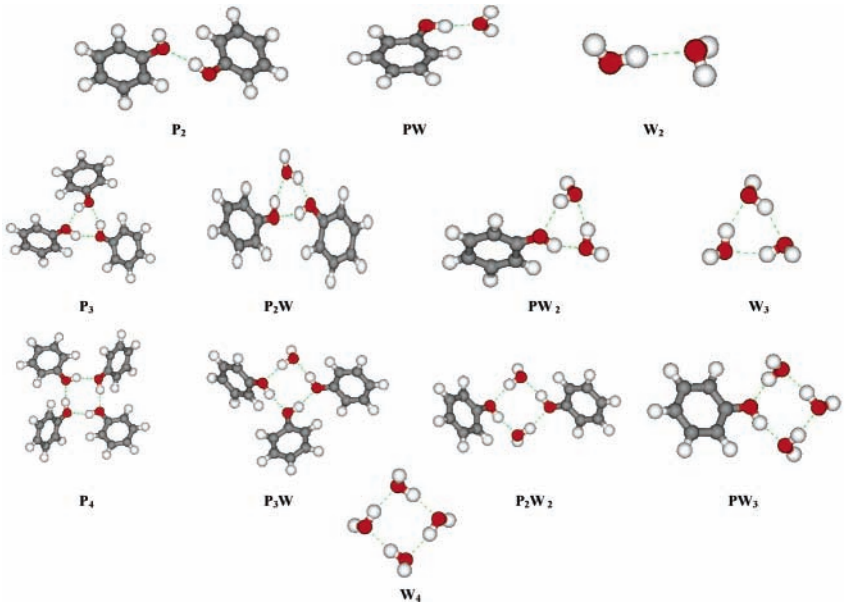

Figure 1. Optimized molecular structure of various phenol, water, and phenol−water clusters.

thereby provides a definition of a chemical bond through bond path and bond critical point (BCP). A BCP is a point at which the gradient vector (∇) of electron density vanishes ($\nabla\rho(\mathbf{r}) = 0$). It is invariably found between two bonded nuclei of a molecule in its equilibrium geometry. Bader[40] has done pioneering work on AIM theory and its applications. Popelier and coworkers have also made noteworthy contributions to further improvement of AIM theory and its applications to various chemical bonding issues.[42−44] Bone and Bader carried out an AIM analysis on several configurations of vdW complexes of Ar with CO_2, C_2H_2, OCS, and SO_2 molecules.[45] Several criteria based on AIM theory have been proposed to characterize hydrogen bonds.[44,46] The cooperative enhancement of inter- and intramolecular hydrogen-bonding interactions in a variety of molecular clusters has also been described using the AIM approach.[47−53] AIM theory has been used to investigate the blue-shifting hydrogen bonds also.[54] The topological descriptors obtained from AIM theory and electron localization function have been employed to distinguish weak, medium, and strong hydrogen bonds in various molecular systems.[45−54] Grabowski used ab initio methods and AIM theory to understand hydrogen bonding in R−C≡N...HF and R−C≡N...HCl complexes.[55] Subramanian et al. [56] have applied AIM theory to understand the interaction of He, Ne, and Ar with HF and HCl. Bader type analysis has been made on di-hydrogen-bonded complexes in the framework of high-level post-Hartree−Fock theory. The success of AIM theory in characterizing hydrogen bonding in various canonical and noncanonical DNA pairs has been demonstrated recently.[57] In the present investigation, hydrogen bonding in phenol, water, and phenol−water clusters has been analyzed with the help of topological and integrated atomic properties of electron density.

Computational Details

The geometries of all P_mW_n clusters were optimized using computationally manageable, meaningfully large basis set 6-31G* at Hartree−Fock (HF), MP2, and density functional theory (DFT) with B3LYP parametrization levels of theory using the G98W suite of programs.[58] Frequency calculations were carried out at HF level and scaled by 0.8929 as is the standard practice.[59] Stabilization energies (SE) of all clusters have been calculated using the supermolecule approach and corrected for basis set superposition error (BSSE) using the counterpoise (CP) procedure suggested by Boys and Bernardi[60]

$$\mathrm{SE} = E_{\mathrm{Cluster}} - \{E_{\mathrm{P}m} + E_{\mathrm{W}n}\} \quad (1)$$

where E_{Cluster} is the total energy of a cluster and $E_{\mathrm{P}m}$ and $E_{\mathrm{W}n}$ are the total energies of phenol and water molecules/clusters calculated using the CP method with the same basis set. The AIM calculations were carried out using the wave functions generated from the ab initio calculations with the help of AIM2000 package.[61]

Results and Discussion

The molecular structure of different P_mW_n clusters as obtained from HF/6-31G* calculations is presented in Figure 1. For water clusters, the O−H bond length varies from 0.9467 Å to 0.9609 Å, while the H−O−H angle varies from 105.49° to 105.76°, in agreement with the previously reported values in the literature.[19] A comparison of the geometrical features reveals that the core structure of hydrogen-bonded phenol clusters and phenol−water mixed clusters is similar to that of water clusters.[20] For the analysis of the strength of hydrogen bonding, |SE|s are considered. The stabilization energies and the number of hydrogen bonds (N_{HB}) in these clusters as determined using the supermolecule approach are listed in Table 1. The |SE| results have been corrected for basis set superposition error. The |SE|s for phenolic clusters are, in general, comparable to those for the corresponding water clusters. A closer examination, however, reveals some interesting features.

The most stable form of water dimer has one O_d−H...O_a hydrogen bond, where d and a refer to the donor and acceptor atoms, respectively, and so does the phenol dimer. In addition, there are two weak C−H...O hydrogen bonds (see Figure 4). These are, in a sense, formed by geometrical constraints. Since the C−O distance in C−H...O is 3.7 Å, it could be considered a weak hydrogen bond. Such a view gets reinforced when we examine the topological characteristics of the electron density map for the system. The MP2 calculation predicts a slightly larger |SE| for P_2 than for W_2, which is presumably because of a larger contribution from the electron correlation (dispersion

TABLE 1: Number of Hydrogen Bonds (N_{HB}) and Stabilization Energies (|SE|) for P_m, W_n, and P_mW_n Clusters as Obtained from Different Levels of Calculation Using 6-31G* Basis Set

	N_{HB}		|SE| (kcal/mol)		
clusters	primary	secondary	HF	MP2	DFT/B3LYP
P_2	1	2	4.3	5.7	4.8
W_2	1		4.7	5.2	5.4
PW	1	1	6.3	7.3	7.7
P_3	3	1	12.8	17.7	15.6
W_3	3		14.1	16.6	18.9
PW_2	3		14.5	17.1	18.9
P_2W	3		13.5	16.8	17.0
P_4	4	4	22.2	31.6	27.9
W_4	4		25.3	30.7	35.2
PW_3	4	1	25.0	30.1	33.6
P_2W_2	4	2	24.9	31.1	32.7
P_3W	4	2	23.6	30.9	30.4

energy), arising from the interaction between the phenyl rings.[16] However, the DFT calculation predicts a slightly lower |SE| for P_2 than for W_2 reflecting the limitations of the predictive power of the B3LYP exchange and correlation functionals.

The mixed dimer of PW can, in principle, exist in two forms: one in which phenol acts as the proton donor and another in which water acts as the donor. Since phenol is more acidic ($pK_a = 10$) than water, it does not come as a surprise that the most stable form of PW has phenol acting as the proton donor, with a |SE| of 6.3, 7.3, and 7.7 kcal/mol, respectively, at HF, MP2, and DFT levels of computation. This includes the strength of an $O_d-H...O_a$ hydrogen bond and a weak secondary $C_d-H...O_a$ interaction (see Figure 4).

While HF and DFT calculations predict a slightly lower |SE| for P_3 than for W_3, MP2 calculations predict a slightly larger |SE| for P_3 than for W_3. The phenolic trimer forms a ring structure very similar to that of the water trimer. Understandably, the three phenyl rings are out-of-plane with respect to each other. The mixed trimers PW_2 and P_2W also show similar three-membered ring structures with comparable stability. The geometries of the trimers are such that there is no room for $C_d-H...O_a$ bond formation. The $C-H...\pi$ type of weak interaction is evident from the topological features corresponding to the phenol trimer.

For the tetramers also, the HF and DFT calculations predict a lower |SE| for P_4 than for W_4. The MP2 calculations, on the other hand, suggest P_4 to have a slightly larger |SE| than W_4. This is in keeping with the presence of four additional weak bonds in P_4 (see Figure 4). In the mixed tetrameric clusters, P_3W has a weak $C_d-H...C_a$ bond and P_2W_2 and PW_3 have $C_d-H...O_a$ bonds with similar |SE| values. The structures of all the clusters P_4, W_4, and P_mW_n ($m + n = 4$) superimposed in Figure 2 show clearly the common core four-membered ring structure.

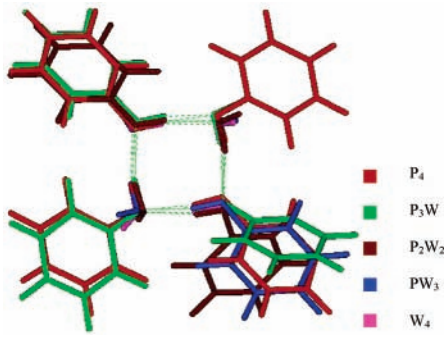

Figure 2. Superimposed structures of P_4, W_4, and mixed phenol−water clusters.

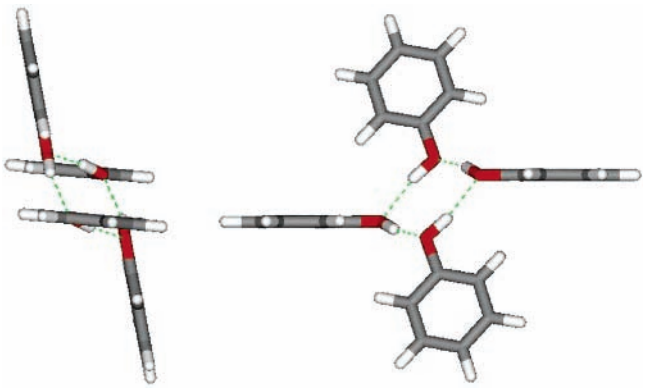

Figure 3. Hydrogen-bonded arrangement of phenol tetrameric cluster.

Hydrogen-bonding distances (Å) in phenol, water, and phenol−water clusters at HF and MP2 levels are listed in Table 2. It can be seen that the $O_d-H...O_a$ bond distance is slightly larger in P_3 and P_4 than in W_3 and W_4, presumably because of the steric hindrance between phenyl groups in the former. The replacement of a water molecule by a phenol molecule in water tetramer increases the $O_d-H...O_a$ intermolecular distance. A similar effect can also been seen in the other mixed clusters. The cluster formed by two water and two phenol molecules shows interesting structural features. The two planar aromatic rings are not parallel to each other and they form a basket type of a structure. In the phenol tetramer, the two aromatic rings are parallel to each other with a reasonable slide as dictated by the hydrogen-bonded core structure and they form a kind of a displaced stacking structure as illustrated in Figure 3. The stacking distance between two phenyl rings is about 3.5 Å, in

TABLE 2: Hydrogen-Bonding Distances (Å) in Phenol, Water, and Phenol−Water Clusters, as Obtained from HF and MP2 Calculations

	range of primary hydrogen bond (OH...O) distances (Å)		range of secondary hydrogen bond distances (Å)	
clusters	HF/6-31G*	MP2/6-31G*	HF/6-31G*	MP2/6-31G*
P_2	2.959	2.879	3.667−3.734 (CH...O)	3.418−3.439 (CH...O)
W_2	2.969	2.927		
PW	2.901	2.848	3.636 (CH...O)	3.487 (CH...O)
P_3	2.867−2.884	2.755−2.798	4.271(CH...π)	3.610 (CH...π)
W_3	2.859−2.876	2.784−2.797		
PW_2	2.813−2. 961	2.746−2.855		
P_2W	2.810−2.934	2.730−2.830		
P_4	2.845−2.858	2.732−2.738	4.207−4.342 (CH...C & CH...O)	3.788−4.331 (CH...C & CH...O)
W_4	2.825−2.826	2.751		
PW_3	2.784−2.901	2.706−2.803	3.556 (CH...O)	3.333 (CH...O)
P_2W_2	2.796−2.868	2.715−2.769	3.595−3.597 (CH...O)	3.394 (CH...O)
P_3W	2.789−2.889	2.711−2.784	3.612−4.188 (CH...O & CH...H)	3.339−3.730 (CH...O & CH...H)

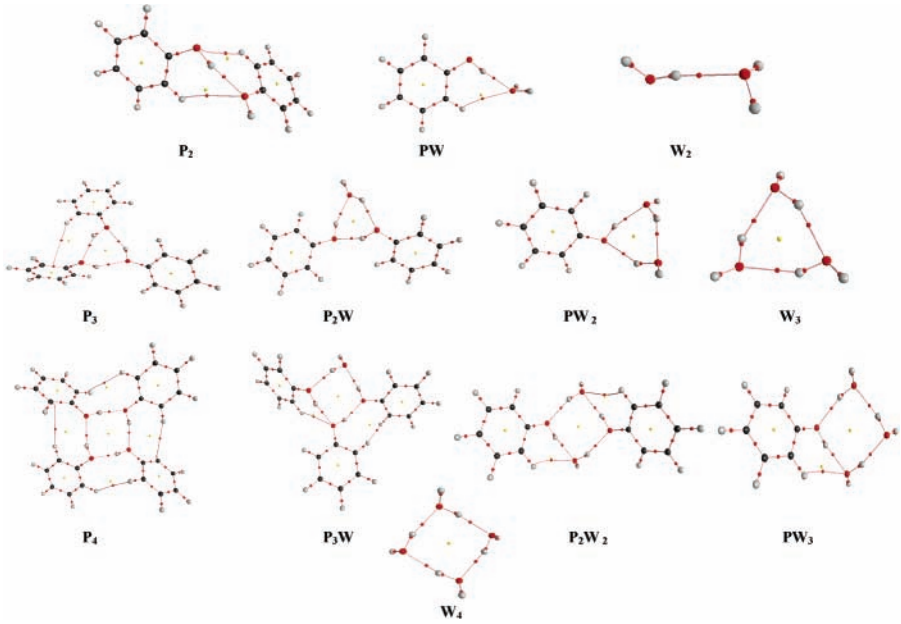

Figure 4. Molecular topography of phenol, water, and phenol−water clusters as obtained from theoretical electron density. Bond critical points are denoted by red dots and the ring critical points by yellow dots.

TABLE 3: Electron Density $\rho(r_c)$ and Laplacian of Electron Density ($\nabla^2\rho(r_c)$) for Various Phenol−Water Clusters

	primary hydrogen bond		secondary hydrogen bond	
clusters	electron density (e/a_o^3)	Laplacian of electron density (e/a_o^5)	electron density (e/a_o^3)	Laplacian of electron density (e/a_o^5)
P_2	0.021	0.019	0.003−0.004	0.004−0.005
W_2	0.021	0.018		
PW	0.025	0.022	0.004	0.005
P_3	0.021-0.022	0.019−0.020	0.002	0.002
W_3	0.022-0.024	0.019−0.020		
PW_2	0.017-0.028	0.015−0.024		
P_2W	0.018-0.027	0.016−0.023		
P_4	0.025-0.028	0.022−0.024	0.002−0.003	0.002−0.003
W_4	0.029	0.025		
PW_3	0.024-0.033	0.020−0.028	0.005	0.005
P_2W_2	0.025-0.032	0.022−0.027	0.005	0.005
P_3W	0.024−0.033	0.021−0.028	0.003−0.004	0.002−0.005

close agreement with the stacking in other $\pi-\pi$ systems and between base pairs in DNA.[62]

AIM Analysis of Hydrogen-Bonded Clusters. The AIM approach is useful in examining the topological features of electron density maps for hydrogen-bonded, di-hydrogen-bonded, and van der Waals complexes.[40−57] The presence of bond critical points has been used as one of the criteria for identifying the presence of hydrogen bonding in any intermolecular complex. The values of $\rho(r_c)$ and $\nabla^2\rho(r_c)$ for the hydrogen bonds present in P_mW_n clusters are listed in Table 3. The existence of C_d−H...O_a type of interaction in some of the clusters is revealed by the presence of additional hydrogen bond critical points and the magnitude of the corresponding topological parameters. The molecular electron density topography of various clusters is shown in Figure 4. The red and yellow dots indicate bond critical points and ring critical points, respectively. It is clear from the figure that there are bond critical points corresponding to the secondary weak hydrogen bonding interaction in P_2, PW, P_3, P_4, P_2W_2, PW_3, and P_3W clusters. It is also clear from Table 3 and Figure 4 that the presence of secondary weak hydrogen bonding adds to the stability of different phenol and phenol−water clusters. The formation of a ring structure in W_3, P_3, and the mixed clusters PW_2 and P_2W is evident from the presence of ring critical points. In phenol trimer, it is possible to identify C−H...π interaction, in addition to the three O_d−H...O_a hydrogen-bonding interactions. In P_4 and the mixed tetramers, the basic O_d−H...O_a hydrogen-bonded core structure is analogous to that of W_4. The existence of the additional C−H...O, weak C−H...C, and C−H...H interaction can be seen in all the mixed clusters.

According to the AIM theory, topological atoms are defined as regions in space consisting of bundle of electron density gradient paths attracted to the nucleus.[40] Because of its firm theoretical footing in quantum mechanics, the AIM theory can be considered as a partitioning scheme to understand the properties of atoms in molecules. Hence, the AIM theory can be used to probe the properties of atoms in intermolecular complexes also. In this study, the integrated atomic properties of hydrogen atoms have been used to understand the nature of hydrogen bonding in various clusters. Cubero et al. have used the AIM theory to distinguish hydrogen bonding from anti-hydrogen bonding and have provided an atomic rationale for the blue shift in anti-hydrogen bonds.[63] Their results showed that the hydrogen-bonding criteria based on the AIM theory are met by the nonconventional di-hydrogen bonding as in C−H...H also. However, they found that to differentiate hydrogen bonding from anti-hydrogen bonding, it is necessary to supplement Popelier's criteria[44] with information on the changes in electron density and other properties of the donor X−H bond, upon complexation. The Popelier criteria[44] used to gain insight into hydrogen bonds include (1) correct topological pattern (bond critical point and gradient path), (2) appropriate

values of electron density at the BCP, (3) proper value of Laplacian of electron density at the BCP, and (4) mutual penetration of hydrogen and acceptor atoms. The criteria pertaining to integrated properties of hydrogen atoms involve (5) an increase of net positive charge, (6) an energy destabilization, (7) a decrease in dipolar polarization, and finally (8) a decrease in atomic volume.

The loss of electron density on hydrogen atoms has been used as one of the criteria for hydrogen bonding. Charges on hydrogen atoms in isolated phenol and water molecules and in the clusters have been computed by integrating the electron density in the appropriate hydrogen atom region partitioned by the AIM theory. The resulting values listed in Table 4 show clearly that the hydrogen nuclei are deshielded upon hydrogen bond formation. The magnitude of this effect ranges from 0.04 to 0.08 au for the different clusters. Similar variations have been observed in previous studies on hydrogen-bonded complexes.[63]

Another property of hydrogen bonding is the energy destabilization of the hydrogen atom, which can be derived from the difference between atomic energies of the hydrogen atoms in the clusters and the isolated molecules. The results presented in Table 4 indicate that this quantity is positive in all the cases and it varies from 0.03 to 0.05 au. It can be seen that hydrogen bond formation necessarily destabilizes the hydrogen atoms that are involved in the bonding.

Popelier had also pointed out that the first moment of the charge distribution, which is a measure of the dipolar polarization, for hydrogen atom decreases upon formation of a hydrogen bond. The first moments for the hydrogen atom in the isolated molecules and in clusters are listed in Table 4. It is clear that hydrogen bonding leads to a decrease in the first moment of hydrogen atoms participating in hydrogen bonding and this decrease ranges from 0.02 to 0.05 au, in accordance with the earlier findings.[44,50]

The decrease in atomic volume of hydrogen upon hydrogen bond formation has also been used as a criterion for hydrogen bonding. The atomic volume corresponding to hydrogen in isolated water and phenol molecules and in clusters of phenol, water, and phenol−water as computed from AIM theory is reported in Table 4. Clearly, there is a decrease in atomic volume of 5−9 au upon formation of hydrogen bond.

Relationship between Total Electron Density and Hydrogen-Bonding Interaction Energy. There are several reports on the use of electron density and its Laplacian as a descriptor to quantify the strength of hydrogen bonds.[46,55,57] It is found that the sums of electron density ($\sum \rho(r_c)$) and its Laplacian ($\sum \nabla^2\rho(r_c)$) at all HBCPs bear a linear relationship with the stabilization energy for all the hydrogen-bonded clusters as illustrated in Figure 5. A linear regression analysis yields

$$\text{stabilization energy} = 212.6 \sum \rho(r_c) \qquad (2)$$

$$\text{stabilization energy} = 248.2 \sum \nabla^2\rho(r_c) \qquad (3)$$

The correlation coefficient is nearly unity in both the cases. It can be seen from Figure 5a and 5b that the hydrogen-bonded clusters having |SE| in the range of 5−25 kcal/mol show three clusters in the density region between 0.020 and 0.125 e/a_0^3 corresponding to the dimers, trimers, and tetramers, respectively. It is interesting to observe from the linear fit that the total density of the phenol and phenol−water mixed clusters is comparable to that of water clusters.

Vibrational Spectral Analysis of Different Clusters. Some of the vibrational frequencies of individual molecules undergo

TABLE 4: Integrated Atomic Properties of the Hydrogen Atoms Involved in Hydrogen Bonding in Different Phenol−Water Clusters and Monomers and the Change (Δ) Arising upon Complexation

	charge (au)			energy (au)			first moment (au)			volume (au)		
clusters	monomer	complex	Δ	monomer	complex	Δ	monomer	complex	Δ	monomer	complex	Δ
P_2	0.6	0.64	0.04	−0.35	−0.32	0.02	0.16	0.13	−0.02	19	13.1	−5.9
W_2	0.59	0.3	0.04	−0. 35	−0.3 3	0.02	0.16	0.14	−0.03	19.6	13.7	−5.9
PW	0.6	0.65	0.05	−0.35	−0.32	0.03	0.16	0.13	−0.03	19	12.3	−6.7
P_3	0.6	0.65	0.05	−0.35	−0.32	0.03	0.16	0.13	−0.03	19	13.2	−5.8
W_3	0.59	0.65	0.06	−0.35	−0.32	0.04	0.16	0.13	−0.03	19.5−19.6	13.1−13.5	−6.0 to −6.5
PW_2	0.59−0.60	0.64−0.66	0.05−0.06	−0.35	−0.31 to −0.32	0.03−0.04	0.16	0.12−0.14	−0.02 to −0.03	19.0−19.6	11.7−15.2	−4.3 to −7.4
P_2W	0.59−0.60	0.64−0.66	0.05 −0.06	−0.35	−0.31 to −0.32	0.03−0.04	0.16	0.13−0.14	−0.02 to −0.03	19.0−19.5	11.8−14.4	−5.1 to −7.3
P_4	0.6	0.66−0.67	0.06	−0.35	−0.31	0.04	0.16	0.12−0.13	−0.03	19	11.4−12.2	−6.9 to −7.7
W_4	0.59	0.66	0.07	−0.35	−0.31	0.05	0.16	0.12	−0.04	19.5−19.6	11.5−11.6	−7.9 to −8.1
PW_3	0.59−0.60	0.65−0.67	0.07−0.08	−0.35	−0.3 0 to −0.31	0.04−0.05	0.16	0.13−0.12	−0.03 to −0.04	19.0−19.6	10.6−12.8	−6.9 to −8.4
P_2W_2	0.59−0.60	0.65−0.67	0.06−0.07	−0.35	−0.30 to −0.31	0.04−0.05	0.16	0.12−0.13	−0.03 to −0.04	19.0−19.5	10.7−12.8	−6.8 to −8.3
P_3W	0.59−0.60	0.65−0.67	0.05−0.08	−0.35	−0.30 − −0.31	0.04−0.05	0.16	0.12−0.13	−0.03 to −0.05	19.0−19.5	10.5−12.8	−6.2 to −9.0

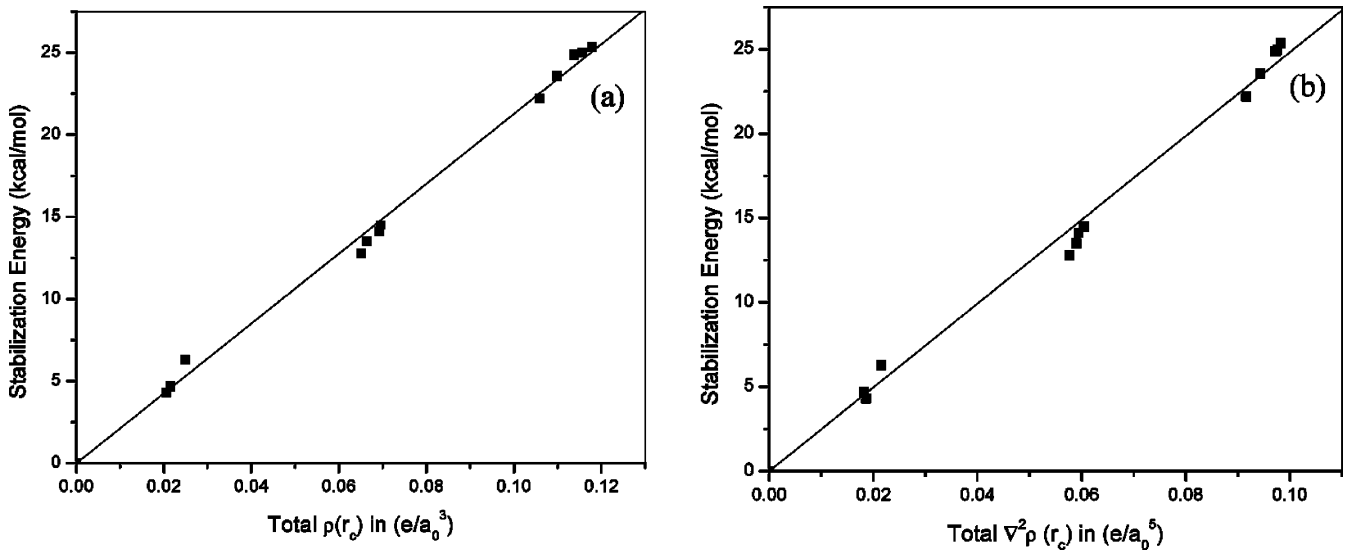

Figure 5. Relationship between stabilization energy (HF/6-31G*) and (a) total $\rho(r_c)$ and (b) total $\nabla^2\rho(r_c)$ for phenol, water, and phenol−water clusters.

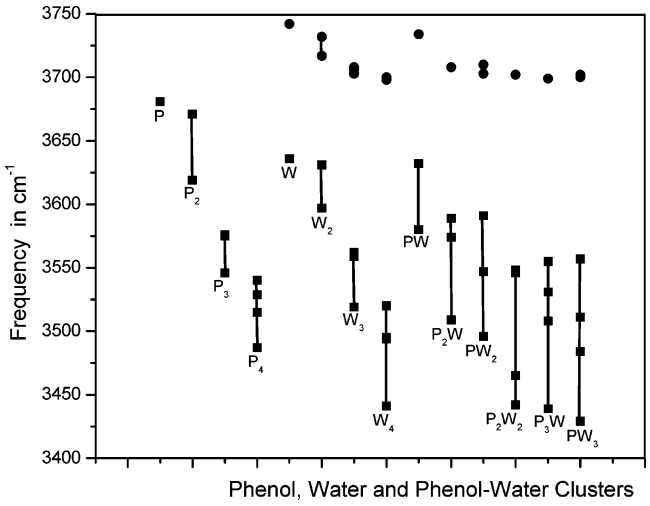

Figure 6. The computed (scaled) vibrational frequencies for OH in P_mW_n, and P_mW_n clusters. In the water molecules, both the symmetric (■) and asymmetric (●) stretches are shown.

substantial shift on complex formation with other molecules.[3,4,7,10] From the changes in the frequencies observed, it is possible to derive information about the characteristics of interaction between molecules. A red shift in the −OH stretching frequencies has been used to characterize hydrogen bond formation. Therefore, vibrational frequencies for isolated water and phenol molecules and their clusters have been calculated at HF/6-31G* level. It is well known that vibrational frequencies calculated at the HF level need to be scaled by a factor before comparison with experiment can be made. The scaled frequencies for −OH stretches in different clusters are presented in Figure 6. Raman and IR spectra show phenolic −OH (ν_{OH}) stretch to occur at 3657 cm^{-1}.[10] The calculated (scaled) frequency at HF/6-31G* level is 3681 cm^{-1} for phenol. In P_2, the calculated ν_{OH} stretches occur at 3619 and 3671 cm^{-1}. The red shift of these modes from that of isolated phenol are 62 and 10 cm^{-1}, respectively. The experimental values corresponding to these vibrational modes are 3654 and 3530 cm^{-1}.[10] Two (see Figure 6) calculated ν_{OH} stretches are obtained at 3576 and 3546 cm^{-1} for phenol trimer. The corresponding red shifts of the bands are 105 and 135 cm^{-1}, larger than that for P_2. The trends in the stretching frequencies are also in reasonable agreement with that of experimental values[10] and indicate the involvement of all the three −OH groups concerned in the hydrogen bonding in the formation of a closed ring structure in P_3. For P_4, four −OH stretching frequencies were obtained and they range from 3487 to 3540 cm^{-1}. The red shift in the ν_{OH} of phenol molecules reinforces the formation of hydrogen bonding and ring structure in P_4.

The calculated stretching frequencies of water clusters and corresponding red shifts upon hydrogen bonding are in good agreement with the earlier reported trends.[19] Since a lot of work has been carried out on structure, stability, and spectra of water clusters, a detailed discussion on the water clusters is not presented here. However, it is very interesting to compare the vibrational frequencies of mixed phenol−water clusters.

The stretching frequencies of the donor and donor/acceptor OH groups participating in hydrogen bonding in the mixed phenol−water clusters range from 3429 to 3632 cm^{-1}. The phenolic −OH stretching frequencies undergo a larger red shift than the water −OH. The free −OH stretching frequencies of water in mixed phenol−water clusters are in the range of that corresponding to isolated water molecules as well as in corresponding water clusters. The formation of a hydrogen bond between the phenolic −OH and a water molecule leads to a red shift of 101cm^{-1} for the phenolic −OH, when compared to the experimentally observed value of 133 cm^{-1}. [10]

The red shift in the vibrational frequencies of the phenolic −OH group in PW_2 is 185 cm^{-1} and the same for P_2W is 172 and 107 cm^{-1}. The −OH stretching mode for the water molecule shows a red shift of 89 and 45 cm^{-1} in the PW_2 complex. For the P_2W complex, the red shift in the water −OH vibrational mode is 47 cm^{-1}.

The red shift in the ν_{OH} of phenol moieties in the complexes having tetrameric core structure ranges from 107 to 252 cm^{-1}. The phenolic −OH group exhibits larger values of red shift in the mixed clusters than in pure phenol or pure water clusters. It is known from previous studies that the increase in red shift is due to increase in donor OH bond length and results in decreased O−O separation in the hydrogen-bonded complexes.[4,7,10] The decrease in computed O−O separation in PW_3, P_2W_2, and PW_3 (see Table 2) is in keeping with the enhanced red shift in the mixed clusters.

Summary and Conclusion

The structure, stability, and spectra of hydrogen-bonded phenol, water, and phenol−water mixed clusters have been investigated using ab initio (HF and MP2) and DFT methods and further probed with the help of AIM theory. While HF and DFT calculations predict the water clusters to have higher |SE| than the corresponding phenol clusters, MP2 calculations suggest the converse to be true. In any case, the mixed clusters have a stability comparable to that of the corresponding water clusters. The usefulness of AIM theory in understanding the hydrogen-bonded phenol, water, and phenol−water clusters has been highlighted in this work. The formation of a hydrogen bond leads to a subtle increase in the electron density at the HBCPs. This increased electron density translates into a greater strength of hydrogen bonding in the clusters. The calculated electron density topological features and integrated atomic properties indicate a reduction in the overall size of the hydrogen atom in the complexed state. The red shift in the OH stretching frequency has been employed as an important tool in probing hydrogen-bonding interactions. Larger red shifts have been noticed for the mixed phenol−water clusters having tetrameric core structures, in keeping with an increase in O−H distances and a decrease in O···O distances.

Acknowledgment. This study was supported in part by a grant from Council of Scientific and Industrial Research, New Delhi, India. R. P. and V. S. are grateful to Dr. T. Ramasami for his continued support.

Supporting Information Available: Optimized geometries (XYZ coordinates) of phenol, water, and phenol−water clusters as obtained from MP2/6-31g* level of calculations. This material is available free of charge via the Internet at http://pubs.acs.org. Details of the optimized geometries of different clusters as obtained from MP2 calculations are available at http://home.iitk.ac.in/~nsath/res_nsath.html.

References and Notes

(1) Jeffrey, G. A.; Saenger, W. *Hydrogen Bonding in Biology and Chemistry*; Springer-Verlag: Berlin, 1991. Jeffrey, G. A. *An Introduction to Hydrogen Bonding*; Oxford University Press: Oxford, 1997.

(2) Desiraju, G. R.; Steiner, T. *The Weak Hydrogen Bond*; Oxford University Press: Oxford, 1999.

(3) Müller-Dethlefs, K.; Hobza, P. *Chem. Rev.* **2000**, *100*, 143.

(4) Brutschy, B. *Chem. Rev.* **2000**, *100*, 3891.

(5) Dessent, C. E. H.; Müller-Dethlefs. K. *Chem. Rev.* **2000**, *100*, 3999. Buck, U.; Huisken, F. *Chem. Rev.* **2000**, *100*, 3863.

(6) Kim, K. S.; Tarakeshwar, P.; Lee, J. Y. *Chem. Rev.* **2000**, *100*, 4145.

(7) Orozco, M.; Luque, F. J. *Chem. Rev.* **2000**, *100*, 4187.

(8) Curtiss, L. A.; Blander, M. *Chem. Rev.* **1988**, *88*, 827. Hobza, P.; Zahradnik, R. *Chem. Rev.* **1988**, *88*, 871. Buckingham, A. D.; Fowler, P. W.; Hutson, J. M. *Chem. Rev.* **1988**, *88*, 963. Hobza, P.; Selzle, H. L.; Schlag, E. W. *Chem. Rev.* **1994**, *94*, 1767. Tomasi, J.; Persico, M. *Chem. Rev.* **1994**, *94*, 2027.

(9) Cramer, C. J.; Truhlar, D. G. *Chem. Rev.* **1999**, *99*, 2161.

(10) Ebata, T.; Fujii, A.; Mikami, N. *Int. Rev. Phys. Chem.* **1998**, *17*, 331.

(11) Chang, H.; Wang, Y.; Lee, T. L.; Chang, H. *Int. J. Mass Spectrom.* **1998**, *279/280*, 91.

(12) Barth, H.-D.; Buchhold, K.; Djafari, S.; Reimann, B.; Lommatzsch, U.; Brutschy, B. *Chem. Phys.* **1998**, *239*, 49.

(13) Hobza, P.; Špirko, V.; Havlas, Z.; Buchhold, K.; Reimann, B.; Barth, H.-D.; Brutschy, B. *Chem. Phys. Lett.* **1999**, *299*, 180.

(14) Bliss, B.; Lommatzsch, U.; Monte, C.; Rettig, W.; Brutschy, B. *Chem. Phys.* **2000**, *254*, 407.

(15) Krauss, O.; Brutschy, B. *Chem. Phys. Lett.* **2001**, *350*, 427.

(16) Hobza, P.; Riehn, C.; Weichert, A.; Brutschy, B. *Chem. Phys.* **2002**, *283*, 331.

(17) Wu, R.; Brutschy, B. *Chem. Phys. Lett.* **2004**, *390*, 272.

(18) Zwier, T. S. *J. Phys. Chem. A* **2001**, *105*, 8827.

(19) Stanley, R. J.; Castleman, A. W., Jr. *J. Chem. Phys.* **1991**, *94*, 7744.

(20) Maheshwary, S.; Patel, N.; Sathyamurthy, N.; Kulkarni, A. D.; Gadre, S. R. *J. Phys. Chem. A* **2001**, *105*, 10525.

(21) Mandziuk, M. *J. Phys. Chem. A* **2004**, *108*, 121.

(22) Kulkarni, A. D.; Babu, K.; Gadre, S. R.; Bartolotti, L. J. *J. Phys. Chem. A* **2004**, *108*, 2492.

(23) Alfonso, D. R.; Karapetian, K.; Sorescu, D.; Jordan, K. D. *J. Phys. Chem. B* **2004**, *108*, 3431. Shin, J.-W.; Hammer, N. I.; Diken, E. G.; Johnson, M. A.; Walters, R. S.; Jaeger, T. D.; Duncan, M. A.; Christie, R. A.; Jordan, K. D. *Science* **2004**, *304*, 1137. Tsai, M.-K.; Jordan, K. D. *J. Phys. Chem. A* **2004**, *108*, 2912. Vila, F.; Jordan, K. D. *J. Phys. Chem. A* **2002**, *106*, 1391. Karapetian, K.; Jordan, K. D. Properties of Water Clusters on a Graphite Sheet. In *Water in Confining Geometries*; Devlin, J. P., Buch, V., Eds.; Springer-Verlag: Berlin, Heidelberg, 2003; pp 139−150.

(24) Feller, D.; Feyereisen, M. W. *J. Comput. Chem.* **1993**, *14*, 1027.

(25) Watanabe, T.; Ebata, T.; Fujii, M.; Mikami, N. *Chem. Phys. Lett.* **1993**, *115*, 347.

(26) Feller, D.; Feyereisen, M. W. *J. Comput. Chem.* **1993**, *14*, 1027.

(27) Oikawa, A.; Abe, H.; Mikami, N.; Ito, M. *J. Phys. Chem.* **1993**, *87*, 1027.

(28) Gerhards, M.; Kleinermanns, K. *J. Chem. Phys.* **1995**, *103*, 7392.

(29) Burgi, T.; Schutz, M.; Leutwyler, S. *J. Chem. Phys.* **1995**, *103*, 6350.

(30) Watanabe, T.; Ebata, T.; Tanabe, S.; Mikami, N. *J. Chem. Phys.* **1996**, *105*, 408. Watanabe, H.; Iwata, I. *J. Chem. Phys.* **1996**, *105*, 420.

(31) Ebata, T.; Fujii, A.; Mikami, N. *Int. J. Mass Spectrom.* **1996**, *159*, 111.

(32) Janzen, Ch.; Spangenberg, D.; Roth, W.; Kleinermanns, K. *J. Chem. Phys.* **1999**, *110*, 9898.

(33) Jansen, Ch.; Gerhards, M. *J. Chem. Phys.* **2001**, *115*, 5445.

(34) Ahn, D.-S.; Jeon, I.-S.; Jang, S.-H.; Park, S.-W.; Lee, S.; Cheong, W. *Bull. Korean Chem. Soc.* **2003**, *24*, 6695.

(35) Dimitrova, Y. *J. Mol. Struct. (THEOCHEM)* **1998**, *455*, 9.

(36) Tsui, H. H. Y.; Mourik, T. V. *Chem. Phys. Lett.* **2001**, *350*, 565.

(37) Benoit, D. M.; Clary, D. C. *J. Phys. Chem. A* **2000**, *104*, 5590.

(38) Benoit, D. M.; Chavagnac, A. X.; Clary, D. C. *Chem. Phys. Lett.* **1998**, *283*, 269.

(39) Yi, M.; Scheiner, S. *Chem. Phys. Lett.* **1996**, *262*, 567.

(40) Bader, R. F. W. *Atoms in Molecules: A Quantum Theory*; Clarendon Press: Oxford, U.K., 1990.

(41) Bader, R. F. W. *J. Phys. Chem. A* **1998**, *102*, 7314.

(42) Popelier, P. L. A. *Atoms in Molecules: An Introduction*; Prentice Hall: New York, 2000.

(43) Popelier, P. L. A. *Coord. Chem. Rev.* **2000**, *197*, 169.

(44) Koch, U.; Popelier, P. L. A. *J. Phys. Chem.* **1995**, *99*, 9747. Popelier, P. L. A. *J. Phys. Chem. A* **1998**, *102*, 1873.

(45) Bone, R. G. A.; Bader, R. F. W. *J. Phys. Chem.* **1996**, *100*, 10892.

(46) Grabowski, S. J. *J. Phys. Chem. A* **2001**, *105*, 10739. Scheiner, S.; Grabowski, S. J.; Kar, T. *J. Phys. Chem. A* **2001**, *105*, 10607. Wojtulewski, S.; Grabowski, S. J. *J. Mol. Struct. (THEOCHEM)* **2003**, *645*, 287. Ranganathan, A.; Kulkarni, G. U.; Rao, C. N. R. *J. Phys. Chem. A* **2003**, *107*, 6073.

(47) Carroll, M. T.; Bader, R. F. W. *Mol. Phys.* **1988**, *65*, 695.

(48) Luque, F. J.; Lopez, J. M.; de la Paz, M. L.; Vicent, C.; Orozco, M. *J. Phys. Chem. A* **1998**, *102*, 6690.

(49) Gonzalez, L.; Mo, O.; Yanez, M. *J. Chem. Phys.* **1999**, *111*, 3855. Espinosa, E.; Molins, E.; Lecomte, C. *Chem. Phys. Lett.* **1998**, 285, 170. Abramov, Y. A. *Acta Crystallogr.* **1997**, *53*, 264.

(50) Peters, M.; Rozas, I.; Alkorta, I.; Elguero, J. *J. Phys. Chem. B* **2003**, *107*, 323 and references therein.

(51) Bader, R. F. W.; Bayles, D. *J. Phys. Chem. A* **2000**, *104*, 5579.

(52) Popelier, P. L. A.; Joubert, L.; Kosov, D. S. *J. Phys. Chem. A* **2001**, *105*, 8254.

(53) Wojtulewski, S.; Grabowski, S. J. *J. Mol. Struct. (THEOCHEM)* **2003**, *621*, 285.

(54) Delanoye, S. N.; Herrebout, W. A.; van der Veken. B. J. *J. Am. Chem. Soc.* **2002**, *124*, 11854. van der Veken, B. J.; Herrebout, W. A.; Szostak, R.; Shchepkin, D. N.; Havlas, Z.; Hobza, P. *J. Am. Chem. Soc.* **2001**, *123*, 12290. Hobza, P.; Havlas, Z. *Chem. Rev.* **2000**, *100*, 4253.

(55) Grabowski, S. J. *J. Mol. Struct. (THEOCHEM)* **2002**, *615*, 239.

(56) Subramanian, V.; Sivanesan, D.; Padmanabhan, J.; Lakshminarayanan, N.; Ramasami, T. *Proc. Indian Acad. Sci. (Chem. Sci.)* **1999**, *111*, 369.

(57) Parthasarathi, R.; Amutha, R.; Subramanian, V.; Nair, B. U.; Ramasami, T. *J. Phys. Chem. A* **2004**, *108*, 3817.

(58) Frisch, M. J.; Trucks, G. W.; Schlegel, H. B.; Scuseria, G. E.; Robb, M. A.; Cheeseman, J. R.; Zakrzewski, V. G.; Montgomery, J. A., Jr.; Stratmann, R. E.; Burant, J. C.; Dapprich, S.; Millam, J. M.; Daniels, A. D.; Kudin, K. N.; Strain, M. C.; Farkas, O.; Tomasi, J.; Barone, V.; Cossi, M.; Cammi, R.; Mennucci, B.; Pomelli, C.; Adamo, C.; Clifford, S.; Ochterski, J.; Petersson, G. A.; Ayala, P. Y.; Cui, Q.; Morokuma, K.; Malick, D. K.; Rabuck, A. D.; Raghavachari, K.; Foresman, J. B.; Cioslowski, J.;

Ortiz, J. V.; Stefanov, B. B.; Liu, G.; Liashenko, A.; Piskorz, P.; Komaromi, I.; Gomperts, R.; Martin, R. L.; Fox, D. J.; Keith, T.; Al-Laham, M. A.; Peng, C. Y.; Nanayakkara, A.; Gonzalez, C.; Challacombe, M.; Gill, P. M. W.; Johnson, B. G.; Chen, W.; Wong, M. W.; Andres, J. L.; Head-Gordon, M.; Replogle, E. S.; Pople, J. A. *Gaussian 98*, revision A.7; Gaussian, Inc.: Pittsburgh, PA, 1998.

(59) Fogarasi, G.; Pulay, P. *Annu. Rev. Phys. Chem.* **1984**, *35*, 191.

(60) Boys, S. F.; Bernardi, F. *Mol. Phys.* **1970**, *19*, 553.

(61) Biegler-Konig, F.; Schonbohm, J.; Derdau, R.; Bayles, D.; Bader, R. F. W. *AIM 2000*, version 1; Bielefeld, Germany, 2000.

(62) Saenger, W. *Principles of Nucleic Acid Structure*; Springer-Verlag: New York, 1984.

(63) Cubero, E.; Orozco, M.; Hobza, P.; Luque, F. J. *J. Phys. Chem. A* **1999**, *103*, 6394.